Int J Adv Manuf Technol (2016) 87:1751–1763
DOI 10.1007/s00170-016-8575-7

ORIGINAL ARTICLE

Comparative thermal analysis of cutting fluids in pendular surface grinding

Marius Winter[1] · **Nadine Madanchi**[1] · **Christoph Herrmann**[1]

Received: 18 August 2015 / Accepted: 1 March 2016 / Published online: 12 March 2016

Abstract The application of cutting fluids in industrial grinding processes is indispensable due to the generated heat in the contact zone. The physical characteristics of the cutting fluid support the cooling and lubrication of the contact zone and can help to prevent heat induced workpiece damages. However, each cutting fluid has different physical properties and therefore the capability to reduce the heat input of the chip removal process into the workpiece varies. This paper investigates the influence of the physical properties of a non-water miscible, mineral oil-based grinding oil in comparison to a water miscible, mineral oil free polymer dilution on the grinding process heat input into the workpiece. The workpiece temperature is determined using an infrared camera and thermocouples whilst conducting the grinding process with cutting fluid. Furthermore, the experimental results are compared with the analytically determined workpiece temperature considering the influence of different models to formulate the convective heat transfer coefficients of the cutting fluid.

Keywords Grinding process · Workpiece temperature · Cutting fluid · Infrared camera · Thermal analysis

✉ Nadine Madanchi
n.madanchi@tu-bs.de

[1] Institute of Machine Tools and Production Technology, Sustainable Manufacturing and Life Cycle Engineering Research Group, Technische Universität Braunschweig, Langer Kamp 19b, 38106 Braunschweig, Germany

1 Introduction

The chip removal process in grinding is based on an enforced sequence of statistically disorderly located single cutting edge engagements with the workpiece surface material [40]. For chip formation, energy is needed in the mechanical processes of cutting, ploughing and rubbing for surface generation. Almost all of the needed specific energy is converted into heat, only a minor part is used to form the material or to accelerate the chips [30]. The generated heat can result in thermal damages, microstructural changes or residual stress in the workpiece surface layer, reducing workpiece quality and life time of the workpiece [2]. To prevent such damages of the workpiece surface layer, cutting fluids are applied. The application of the cutting fluid reduces the heat input into the workpiece based on its cooling and lubricating capabilities.

Yet, each cutting fluid has, depending on its composition, different cooling and lubricating capabilities. The commonly used non-water miscible fluids (e.g. mineral oil based grinding oils) have a very good lubricating capability, but an insufficient cooling capability, whilst the opposite characteristic applies for water miscible fluids (e.g. mineral oil based emulsions). Further disadvantages of mineral oil-based fluids are their dependence on a non-renewable resource as well as the environmental impacts over the lifecycle as well as concerns regarding occupational health during use [9]. To overcome these drawbacks, alternative cutting fluids can be applied, which combine a good lubrication and cooling capability. Biopolymers diluted in water can be such an alternative. Technological, economic and environmental investigations regarding the application of this alternative cutting fluid showed promising potentials when applied for instance in grinding [41, 42].

To evaluate these combined cooling and lubricating capabilities, a comparative analysis on the application of the polymer-based dilution and a mineral oil-based grinding oil in pendular surface grinding has been conducted. The focus is on the workpiece temperature to examine and to predict the cooling capabilities of the polymer based cutting fluid in comparison to a mineral oil based cutting fluid. For this purpose, two different measuring techniques are conducted by the application of an infrared camera and thermocouples. Furthermore, to predict the workpiece temperature, a thermal analysis is conducted considering the properties of the polymer based dilution.

A brief overview of different techniques of temperature measurement is presented in chapter 2, followed by the influence of the cutting fluid on the temperature. Chapter 3 discusses the methodological procedure, materials used and the experimental setup to determine the workpiece temperature using an infrared camera and thermoelements. Furthermore, the chapter presents the used formulations to predict the workpiece temperature. In chapter 4, the observed and predicted results are presented and discussed.

2 Research background

2.1 Temperature measurement in grinding

To evaluate the influence of the heat input of the grinding process into the workpiece and the possible implications on the workpiece quality (e.g. the geometrical accuracy, the homogeneity of material properties, etc.), the knowledge of the workpiece temperature is crucial. However, the measurement of the temperature in the contact zone between grinding wheel and workpiece is particularly challenging. The reason is a moving heat source and therefore changing temperature fields and gradients within the workpiece. Furthermore, in wet grinding, a constant cutting fluid supply limits the accessibility [11]. Thus, different methods for temperature measurement have been developed. An overview is presented in Fig. 1. Basically, temperature measurement techniques can be distinguished with regard to the principle of heat transfer between heat source and measuring device. They either use the principle of heat conduction (a direct contact measurement) or heat radiation (a non contact measurement).

Thermocouples belong to the group of heat conduction based methods and are the preferred technique for temperature measurement in grinding [33]. Thermocouples use the Seebeck effect and consist of two different materials, which are connected at two measuring points. If these two measuring points have different temperatures (T_1, T_2), a voltage (U) is tapped which is proportional to the original temperature difference. The thermo voltage is described by

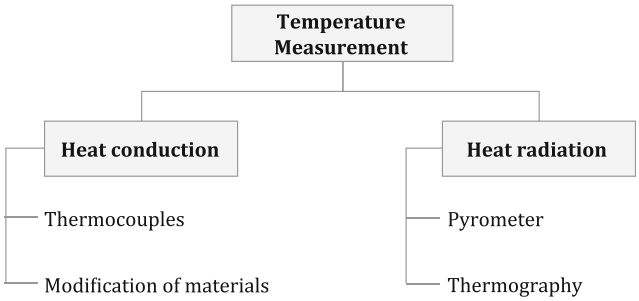

Fig. 1 Temperature measurement techniques in grinding based on [24, 34]

$$U = k^*(T_1 - T_2) \quad (1)$$

with k as the Seebeck coefficient. The value depends on the material matching and average working temperature [34]. Thermocouples can either be implemented as a single-wire or as a two-wire method. Both methods mainly differ regarding the use of the workpiece within the experimental setup. In the one-wire method, the workpiece and the wire form the thermocouple and are used as the measuring elements. This relationship between workpiece and wire does not exist in the two-wire method [7]. Instead of wire, it is also possible to use an insulated foil to form the thermocouple. In the single-pole technique, the wire or thermo foil can be inserted either in the grinding wheel or the workpiece. An insertion in the grinding wheel, however, is more complicated and therefore less popular for experimental purposes [2]. It can further be distinguished between an open and a closed circuit. Usually, the open circuit is applied and an insulated wire (single-wire method) or two insulated wires (two-wire method) are inserted in a prepared workpiece and positioned at the workpiece surface. During grinding, a measuring junction is formed, and the temperature is measured directly in the contact zone. In the case of the closed circuit, the thermocouples are inserted below the workpiece surface. Thus, it is possible to measure the temperature at different distances from the contact zone, but this may also lead to inaccuracies [2]. For the single-wire method, a permanent contact between wire and workpiece is achieved by welding or brazing [33]. The different techniques of thermocouples are widely documented in literature and have to be selected individually for each application. Black et al. compared the performance of single- and two-wire methods in grinding. The authors showed that a smaller measurement junction improves the temperature response for the single-wire method. This result is valid under dry and wet grinding conditions [3]. A comparison by Xu and Malkin showed that closed two-wire thermocouples and foil/workpiece thermocouples give comparable temperature responses under dry grinding conditions [44] Batako et al. showed that a thin, but wide film single-pole thermocouple provides a

more reliable temperature profile under wet grinding conditions [2].

Another heat conduction-based method uses PVD coatings with a low melting point such as indium, bismuth and heat-sensitive paints [2]. This method measures the temperature indirectly, based on the modification of materials ot coatings due to the influence of heat. The inner surface of a split workpiece is coated perpendicularly to the ground surface with different coatings. As each coating melts at a known temperature, it is possible to draw a conclusion on the maximum temperature below the finished surface [30]. Thus, the technique provides a temperature response very closely at the direct contact zone. Another advantage is the unrestricted application under wet grinding conditions and also for very high grinding temperatures. With this technique, it is only possible to determine the maximal temperature of the grinding process. Furthermore, the coating has to be exposed to high temperatures for a certain amount of time in order to melt. Thus, short-term changes in temperature cannot be measured with this technique [26]. However, this technique provides a useful cross-cheque on the maximal measured temperature of other measurement techniques [2]. Kato et al. used this coating technique to measure the temperature in grinding processes. Using different coatings, Kato showed that an increasing distance from the contact zone leads to decreasing temperatures [16]. Comley et al. used a thin 0.2-μm film of low melting point PVD coatings to measure the temperature for high efficiency deep grinding (HEDG) and determined a temperature trend for increasing material removal rates [8].

Besides the direct contact measurements, there is a group of non-contact measurements using the technique of heat radiation (Fig. 1). The workpiece temperature is measured using infrared pyrometers. For this purpose, the radiation transmitted from an object is determined. As each object transmits radiation, it is also possible to measure the temperature of working grains on the grinding wheel just after their engagement with the workpiece surface [35]. The pyrometer detects the radiation of the measured object. By comparing the radiation with the standard radiation of a so-called black object, it is possible to assign the specific temperature to the radiation. By using an infrared pyrometer, it is possible to measure very small objects with rapidly changing temperatures such as cutting grains [36]. Since this technique measures the temperature from outside the contact zone, the measured temperature may be significantly lower than the temperature at the contact zone because of heat emissions and heat conduction inside the workpiece. The use of cutting fluid and accessibility to the contact zone poses further challenges to the use of pyrometers [33]. Ueda et al. used this technique to measure the temperature of single cutting grains some milliseconds after cutting. The study showed that the average grain temperature decreases with an increasing wheel speed [36].

The other heat radiation-based temperature measurement technique uses thermography. An infrared camera is oriented perpendicularly to the surface of the target object and records its radiated energy. In contrast to the pyrometer, the radiation is converted into a thermal image of the whole temperature field [2, 32]. The technique provides a graphic image in real-time and does not need a physical attachment to the workpiece. However, similar to the pyrometer, the same restrictions regarding the use of cutting fluid and accessibility to the contact zone apply for the use of an infrared camera. Therefore, the application of this temperature measurement technique is mainly limited to dry grinding [24]. Lange and Weber, however, prepared an experimental setup and enclosed the infrared camera to protect it from cutting fluid and swarf [17, 39]. With this setup, the authors determined the workpiece temperature distribution in wet surface grinding. Anderson et al. used an infrared camera to validate predicted temperatures of a thermal model with actual temperatures determined in dry grinding experiments. The set-up included a miniature black body to calibrate the infrared camera before each experiment [1].

Generally, all of the previously presented methods are suited for temperature measurements in grinding. However, rapidly changing temperatures with significant temperature gradients and a limited accessibility complicate the temperature measurement. As shown, the different techniques have specific characteristics with advantages and disadvantages. Based on classifications made by Schwarz and Denkena, Fig. 2 summarizes the review and evaluates the temperature measurement techniques regarding the application in grinding processes [11, 32].

Temperature measurment techniques	Criteria				
	Use of cutting fluid	Response time	Workpiece preparation	Reproducibility	Costs
Thermocouple	●	◐	◔	○	◕
Coating technique	●	○	◔	◔	◕
Pyrometer	◔	◕	◔	◐	◔
Thermography	◔	●	◕	◐	○
Degree of fullfilment	very poor ○	poor ◔	medium ◐	good ◕	very good ●

Fig. 2 Classification of temperature measurement techniques in grinding processes (based on [11, 32])

As the use of cutting fluid is essential in grinding, this criterion evaluates if the technique is suited for wet grinding. The response time describes the availability and resolution of the recorded data. Since the accessibility is limited, the need for workpiece preparation considers the effort for the experimental setup. The reproducibility describes the additional effort for further experiments. The criteria costs evaluate the financial effort to realise the different temperature measurement techniques. Overall, the classification shows that the type of temperature measurement techniques has to be selected individually with regard to the requirements of the specific grinding process.

2.2 Influence of the cutting fluid on the workpiece temperature

Compared to other machining processes, the temperatures in grinding processes are comparably high, with locally and temporally limited temperature peaks capable of causing workpiece damages [30]. For example, in case of workpieces produced of 1.3505 bearing steel, Rowe reports that residual stress typically occurs at transition temperatures of 400 °C. The exceedance of 450 °C typically causes temper damages and temperatures above 850 °C typically cause re-hardening damages [30]. Therefore, it is important to prevent thermally related geometrical deviations (e.g. form and accuracy errors) as well as changes of the surface and material integrity (e.g. thermal damage, micro-structural changes and residual stress). An option in this context is the application of cutting fluid.

The cutting fluid influences the temperature of a workpiece by its three main tasks: lubricating, cooling and cleaning. The lubricating capability of the applied cutting fluid influences the friction between the abrasive grain and workpiece surface. Due to a reduced friction, the connected heat generation decreases as well [38]. The cooling capability of the cutting fluid influences the heat conduction; instead of the conduction into the workpiece, the heat is conducted into the cutting fluid [37]. And the cleaning capability of the cutting fluids can influence the grinding wheel cleanliness to prevent wheel clogging and therefore an increase of the heat input into the workpiece due to an inclined friction [14].

Besides the lubrication capability, especially the cooling capability, has a major influence on the workpiece temperature. To evaluate the cooling capability of a cutting fluid the physical fluid properties, including specific heat capacity (c_p), heat conductivity (λ) and vaporization heat (ΔQ_v), can be used [38]. Table 1 shows the corresponding physical properties for commonly used water-based and non-water-based fluids. In comparison to non-water-based fluids (e.g. mineral oil), the water-based fluids can absorb more heat before a temperature change occurs. The water-based fluids also have a significantly higher heat conductivity resulting in a higher heat transfer rate and lower heat accumulation. Furthermore, the water-based fluids have a higher heat of vaporization (by the factor of ten), resulting in a higher heat absorption when changing from the liquid to the gaseous state.

Table 1 Physical properties of water and mineral oil [38]

Physical properties	Water	Mineral oil
Specific heat capacity, c_p [J/(g·K)]	4.19	1.67
Heat conductivity, λ [W/(m·K)]	0.56	0.13
Heat of vaporization, ΔQ_v [J/g]	2260	210

Investigations examining the cutting fluid influence on the workpiece temperature in grinding processes have been conducted by several authors over the last decades. The influence of the cutting fluid type and strategy on the grinding process and the modelling of the fluids impact on the process, have been main focus of these investigations.

Dederichs, for example, investigated the influence of mineral oil based emulsion and grinding oil in surface grinding of different workpiece material types on the temperature in the workpiece peripheral zone [10]. Yasui and Tsukuda as well as Ohishi and Furukawa examined in their investigations of pendular and deep grinding processes the influence of the application of grinding oil and a water-miscible solution [27, 45]. Besides the different cooling behaviours of these two cutting fluids, these studies showed the influence on the cooling effect when the film boiling temperature of the fluid is exceeded. The study of Ohishi and Furukawa indicates a film boiling at a temperature of about 100 °C for the water miscible solution and of about 300 °C for the grinding oil [27]. The film boiling results in a reduction of the cooling effectiveness leading to a workpiece temperature rise [20].

Motivated by the aim to reduce the amount of cutting fluid and resource consumption, investigations were conducted for example by Langemeyer, Maiz as well as Hadad and Sadeghi. Langemeyer examined the cooling influence of flood lubrication, applying different cutting fluids (mineral oil based emulsion as well as grinding oil on mineral oil and palm oil basis) in comparison to the influence of minimal quantity lubrication (MQL) in pendular and deep grinding [18]. The focus of Maiz was the application of liquid nitrogen, MQL and a mineral oil-based emulsion as a cooling medium in pendular and deep grinding [22]. Hadad and Sadeghi conducted a thermal analysis of pendular grinding and investigated the cooling influence of five different MQL fluids in comparison with grinding processes without (dry) and a flood lubrication [12]. The results of these investigations showed a promising potential of the application of MQL and liquid nitrogen to reduce

the amount of needed cutting fluid. Yet, limiting factor of these strategies were the attainable material removal rates before a thermal damage of the workpiece occurred.

Besides the application of MQL, liquid nitrogen (or other cryogenic liquids) or no cutting fluid at all, a further option is the adjustment of the cutting fluid supply in flood lubrication. For example, Wittmann investigated the influence of the flood lubrication strategy on the workpiece temperature in dependence of the fluid supply parameters (pressure and volume flow) and nozzle type (tangential nozzle and shoe nozzle) [43]. The results of this investigation showed the potential of improved flood lubrication, due to a lower workpiece temperature and realization of higher material removal rates.

The modelling of the workpiece temperature has been comprehensively investigated and described by several authors in the last decades. Common basis for most physical temperature models in grinding are the works of Carslaw and Jaeger for a moving heat source [6, 15]. On this foundation, Outwater and Shaw were the first to apply this model for the thermal analysis of a grinding process [28]. The model was further developed by Hahn, due to the consideration of the heat source created by the grain wear flat [13]. Takazawa simplified the approach by the presentation of an approximation equation, and comprehensive models were independently presented by Rowe, Lavine or Malkin and Guo, allowing to consider the heat flows into tool, workpiece, cutting fluid and chips [19, 23, 30].

3 Methods and materials

3.1 Methods

In the following, the used measuring methods to determine the workpiece temperature are presented. To obtain the workpiece temperature two different measuring methods were realized. The first method is based on the measurement of the heat radiation using an infrared camera. The second method is based on the application of thermocouples to determine the workpiece temperature due to heat conduction. Both methods were realized to cross-cheque the accuracy of each measurement method. Additionally, the equations to theoretically calculate the workpiece temperature using the formulations presented by Rowe [30] and Marinescu et al. [25] are applied. However, works of Black, Zhang et al. and Lin et al. have also been considered. This step was conducted to evaluate the influence of the different physical cutting fluid properties of the polymer based dilution and the grinding oil also theoretically.

3.1.1 Temperature measurement using an infrared camera

Figure 3 shows the experimental setup to determine the workpiece side-plane temperature field using an infrared camera. The camera (model InfraTec VarioCAM hr inspect 720 S) was mounted to the machine table via a protective case and the camera lens faced the workpiece side-plane. The case was necessary to protect the infrared camera against cutting fluid and grinding swarf. The inner surface of the protective case was blackened to prevent possible reflections. The workpiece was fixed to the protective case (see Fig. 3b), and gaps were caulked with sealing compound.

Prior to the grinding experiments the workpieces were prepared with a defined ridge at the workpiece side-plane (thickness of 1 mm) to guarantee the leak tightness of the protective case against the cutting fluid (see Fig. 3b). The infrared camera measured the heat radiation emitted by the side-plane surface at the workpiece. For this purpose, the heat radiation at the workpiece side-plane was continuously scanned with a frequency of 50 Hz and a resolution of 640 × 480 pixels within a measuring window (height 16 mm, width 76.5 mm). The

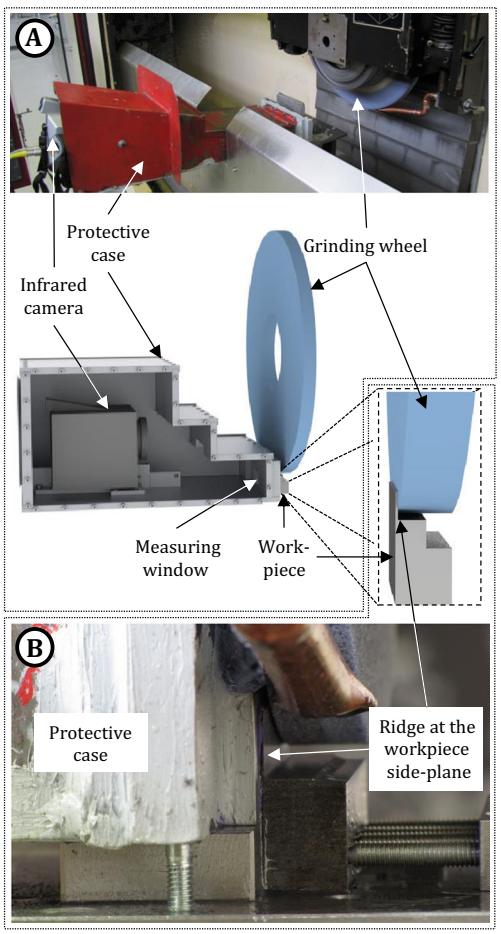

Fig. 3 Experimental setup for workpiece temperature measurement using an infrared camera. **a** Overview of the setup in the workspace. **b** Close view on the contact zone

measured heat radiation is directly influenced by the emissivity of the measured surface. To obtain a constant surface emissivity, the workpiece side-plane was coated with a heat resistant black colour (see Fig. 3a). To determine the heat emissivity, the workpiece was heated in an oven for about 1 h to a specific temperature and then the temperature of the coloured workpiece side-plane was measured with the infrared camera. Afterwards, the measured temperature and the workpiece temperature were compared and the emissivity determined. This procedure was repeated three times with different oven temperatures (100, 200 and 250 °C). The emissivity of the coloured side-plane was determined with $\varepsilon = 0.85$.

The infrared camera was connected to a personal computer, and the measured thermal images were continuously recorded using the software IRBIS 3 Plus® by InfraTec.

3.1.2 Temperature measurement using thermocouples

A further option to measure the workpiece temperature, besides the application of an infrared camera, is the use of thermocouples within the workpiece. The experimental setup to measure the workpiece temperature using thermocouples is presented in Fig. 4.

Three thermocouples (two-wire method) were consecutively placed in grinding direction grinding, within eroded through holes inside the workpiece. Prior to each grinding trail, the thermocouple position was adjusted in such a manner that the top of each thermocouple was placed just below the workpiece surface created by the last grinding stroke (see Fig. 4b). To improve the heat flow from the workpiece to the thermoelement, thermal conductance paste was applied into the eroded holes. For the measurement of the workpiece temperature, type K thermocouples with a measuring range of −200 to 1.250 °C were applied. The used thermocouples were calibrated prior to their application using a liquid with a defined temperature.

To measure the temperature inside the workpiece, the following measuring chain was configured. The signals of the thermocouples were transformed in a proportional voltage output signal. This output signal was filtered using a Bessel low pass filter (fourth order) with a frequency of 3 Hz. The filtered signal was recorded by an analogue-digital converter from National Instruments on a standard laptop PC with a LabView®-based data acquisition and processing software.

3.1.3 Calculation of the workpiece temperature

The average workpiece temperature (T_w) can be formulated based on the partition ratio between the workpiece and the grain (R_{ws}), the total heat flow (q_t), the heat flow into the chips (q_{ch}), the heat transfer coefficient of the workpiece (h_w) and the fluid ($h_{f,x}$) and the ambient temperature (T_a) [25, 30]:

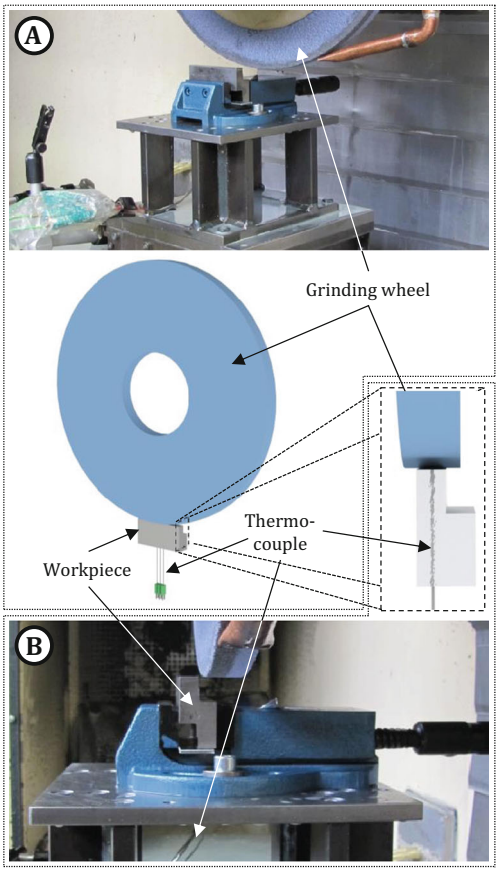

Fig. 4 Experimental setup for workpiece temperature measurement using thermocouples. **a** Overview of the setup in the workspace. **b** Close view on the contact zone

$$T_w = \frac{R_{ws} \cdot (q_t - q_{ch})}{h_w + h_{f,x}} + T_a \tag{2}$$

The total heat flow (q_t) comprises the heat flow into the workpiece (q_w), chips (q_{ch}), cutting fluid (q_f) and grinding wheel (q_s) (see (Eq. 3)) [30]. The q_t can be described based on the needed cutting power (P_c) for chip formation, the grinding width (b_s) and the effective cutting length (l_e):

$$q_t = q_w + q_{ch} + q_f + q_s = \frac{P_c}{b_s \cdot l_e} \tag{3}$$

The heat flow into the chips can be formulated using the estimated melting temperature of the generated chips (T_{ch}) whilst considering density (ρ_w) and specific heat conductivity (c_w) of the workpiece as well as the cutting depth (a_e), the workpiece velocity (v_w) and the effective cutting length (l_e) [30]:

$$q_{ch} = \rho_w \cdot c_w \cdot T_{ch} \cdot \left(\frac{a_e \cdot v_w}{l_e} \right) \tag{4}$$

To determine R_{ws}, a steady-state solution (Eq. 5) or a transient-state solution (Eq. 6) can be used. The difference

between both solutions is the consideration of a dimensionless time parameter to consider the grain contact behaviour along the contact length. Therefore, the transient solution allows to evaluate the partition ratio at each point in the contact zone [4].

The steady-state solution of the R_{ws} for an assumed circular grain contact of the effective contact radius (r_o) further includes the grinding wheel velocity (v_s), the grain heat conductive (λ_g) and the thermal properties of the workpiece $\beta_w = \sqrt{\lambda_w \cdot \rho_w \cdot c_w}$ (heat conductive (λ_w), density (ρ_w) and specific heat capacity (c_w) of the workpiece):

$$R_{ws} = \left(1 + \frac{0.974 \cdot \lambda_g}{\beta_w \cdot \sqrt{r_o \cdot v_s}}\right)^{-1} \tag{5}$$

The transient-state solution (Eq. 6) extends the steady-state solution from (Eq. 5) by the consideration of the transient function ($\Phi(\tau)$) [4]:

$$R_{ws} = \left(1 + \frac{0.974 \cdot \lambda_g}{\beta_w \cdot \sqrt{r_o \cdot v_s}} \cdot \frac{1}{\Phi(\tau)}\right)^{-1} \tag{6}$$

To determine the transient function, Black presented an exact and a simplified solution [4]. However, the simplified solution (presented in (Eq. 7)) allows to represent the transient behaviour with sufficient accuracy.

$$\Phi(\tau) = 1 - e^{\left(\frac{-\tau}{1.2}\right)} \tag{7}$$

The dimensionless time (τ) can be determined based on the thermal diffusivity of the grain (α_g), the effective cutting length (l_e), the effective contact radius (r_o) and the grinding wheel velocity (v_s) (Eq. 8) [4]. $\alpha_g = (\lambda_g/(\rho_g \cdot c_g))$ enfolds the grains' heat conductivity (λ_g), density (ρ_g) and specific heat capacity (c_g).

$$\tau = \frac{\alpha_g \cdot l_e}{r_0^2 \cdot v_s} \tag{8}$$

According to Black, the steady-state solution should be used when $\tau > 5$ and the transient-state solution when $\tau < 5$ [4], due to the reason that the determined R_{ws} is more accurate within those limits.

The effective contact length (l_e) was determined in accordance with Brandin, based on the cutting depth (a_e), the achieved surface roughness (R_z) and the grinding wheel diameter (d_s) [5, 31].

$$l_e = \sqrt{(a_e + R_z) + d_s} + \sqrt{(a_e + R_z)} \tag{9}$$

To approximate the effective grain contact radius, Zhu et al. proposed a formulation considering the cutting depth (a_e) and the abrasive cone angle (θ) Zhu et al. [47].

$$r_0 = a_e \cdot tan\left(\frac{\theta}{2}\right) \tag{10}$$

The heat transfer coefficient of the workpiece (h_w) can be formulated using the thermal properties of the workpiece (β_w), a constant (C) derived from the Peclet number [25], the workpiece velocity (v_w) and the effective cutting length (l_e).

$$h_w = \frac{\beta_w}{\mathrm{C}} \cdot \sqrt{\frac{v_w}{l_e}} \tag{11}$$

In order to consider the cooling properties of the cutting fluid, the convective heat transfer coefficient of the fluid (h_f) is of major importance. In literature, two different approaches to determine the coefficient are presented by Rowe and Zhang et al. [30, 46]. The approaches vary regarding the degree of the considered geometrical and physical relationships. Therefore, in the following, the two different approaches are considered to determine the heat transfer coefficient of the fluid. Furthermore, the determination of the convective heat transfer coefficient based on experimental values is presented. The different approaches to determine the convective heat transfer coefficient are represented by $h_{f,\,x}$ (with x for the approaches presented by Rowe, Zhang and experimental).

The approach presented by Rowe is based on the assumption that the entire effective contact area between workpiece and grinding wheel is covered with cutting fluid [30]. Therefore, this approach is also known as "fluid wheel model", comprising the thermal properties of the cutting fluid (β_f), the grinding wheel velocity (v_s) and the effective cutting length (l_e).

$$h_{f,\,Rowe} = \beta_f \cdot \sqrt{\frac{v_s}{l_e}} \tag{12}$$

Zhang et al. proposed a "laminar flow model" based on the works of Lin et al. to determine the convection heat transfer coefficient based on the principles of applied fluid dynamics and heat transfer [21, 46]. The model considers the density (ρ_f), the specific heat capacity (c_f), the dynamic viscosity (η_f) and the heat conductivity (λ_f) of the fluid as well as the grinding wheel velocity (v_s) and the effective cutting length (l_e).

$$h_{f,\,Zhang} = \frac{4}{9} \cdot \rho_f^{\frac{1}{2}} \cdot c_f^{\frac{1}{3}} \cdot \eta_f^{-\frac{1}{6}} \cdot \lambda_f^{\frac{2}{3}} \cdot \sqrt{\frac{v_s}{l_e}} \tag{13}$$

A further option is the experimental determination of the convection heat transfer coefficient based on the transformation of (Eq. 2).

$$h_{f,\,exp} = \frac{R_{ws}\cdot(q_t - q_{ch})}{T_w - T_a} - h_w \tag{14}$$

3.2 Materials

3.2.1 Grinding machine, grinding wheel and grinding conditions

The grinding experiments were conducted using a Blohm Profimat 307 surface grinding machine. The machine tool's maximal spindle power was 27 kW and the maximal table feed was $v_w = 60,000\ mm/min$.

The used vitrified bonded aluminium oxide (Al_2O_3) grinding wheel had a high porosity and a permeable structure. The wheel featured a cylindrical shape with a straight profile, the external tool diameter was 350 mm and the tool width was 20 mm (specification 93 A 46 H8A V217). The physical properties were approximated based on the values given by Marinescu et al. Accordingly, for an Al_2O_3 abrasive grain, the following values were used for the heat conductive ($\lambda_g = 35.0$ W/(m·K)), the density ($\rho_g = 3,980.0$ kg/m^3) and the specific heat capacity ($c_g = 765.0$ J/(kg·K)) [25].

The cutting speed of the grinding wheel was $v_c = 35 m/s$ and the workpiece speed was $v_w = 0.5\ m/s$. For each cutting fluid, four experimental series were performed, which differed in regard to the used cutting depth ($a_e = 5; 10; 15\ and\ 20\ \mu m$). The cutting width was 10 mm and at each cutting depth a specific volume of material removed by cutting of $V'_w = 200\ mm^3/mm$ was removed. Each cutting depth was repeated three times. Between each repetition, the grinding wheel was dressed with an infeed of $a_{ed} = 10\ \mu m$ and a traverse dressing speed of $v_{fad} = 50.5\ mm/min$ using a diamond form roll (specification 1 SG 71P 130–0.4).

3.2.2 Cutting fluid and workpiece

A mineral oil-based grinding oil and a water miscible polymer dilution were tested during the experiments as cutting fluids. The physical properties of both cutting fluids are presented in Table 2. The cutting fluids were applied into the contact area via a tangential nozzle.

The workpiece material consists of hardened carbon alloy steel with the designation 1.3505 (DIN 100Cr6). The material has a surface hardness of 527 HV 5 and features a cuboid shape with a length of 83.4 mm. To calculate the chip temperature (T_{ch}) the maximum chip energy at the melting point was assumed with $e_{ch} = 6\ J/mm$ [25]. The used properties of the workpiece are presented in Table 3.

3.2.3 Measurement devices

The cutting power was measured by a three-phase power analyzer (Load Controls® PPC-3) with a temporal resolution of 15 ms. The signals from the power metre were recorded via a LabView®-based data acquisition and processing system. The surface roughness (R_z) was measured at four different points on the workpiece by a surface measurement device (Hommel-Etamic® T1000 basic). The workpiece temperature was measured using an infrared camera and thermocouples. The experimental setups for both measuring techniques are presented in section 3.1.

4 Results and discussion

4.1 Experimental results

Figure 5 presents the results obtained by the infrared measurement of the workpiece side-plane maximal and mean temperature field during the grinding process. The thermographic images on the left side show the measured maximal workpiece temperature for the application of the grinding oil and the polymer dilution at the four different cutting depths. The thermographic images on the right side show the corresponding observed mean workpiece temperature. In every thermographic image, the maximal or mean workpiece temperature is presented with a small triangle. Furthermore, the position of the grinding wheel and the workpiece level is indicated in each thermographic image in dashed lines. The direction of the grinding wheel movement is from right to left in every image.

The differentiation between mean and maximal temperature shows the influence of a sufficient and insufficient cutting fluid supply of the grinding gap. The highest workpiece temperature was always measured in each thermographic image on the right side. This is due to the application of only one cutting fluid nozzle on the right side of the grinding wheel (see Figs. 3 and 4). This configuration has the drawback that during the first seconds of engagement an insufficient cutting fluid supply occurs (see Fig. 5 chart (A)). In this configuration, the cutting fluid is only conveyed against the workpiece side and not into the contact zone. A sufficient cutting fluid supply is ensured in the middle and on the left side of the workpiece (see Fig. 5 chart (B)). Accordingly, the mean workpiece temperature is lower compared to the maximal temperature. A further drawback of this configuration is an accumulation of heat on the right side of the workpiece. If the cutting depth is higher, then the heat input and therewith the accumulation would increase as well, which could result in thermal damages or stresses within this particular workpiece area. To overcome this drawback, an additional cutting fluid nozzle needs to be integrated on the left side of the grinding wheel, and the

Table 2 Properties of the cutting fluids

Property	Symbol	Unit	Grinding oil	Polymer dilution
Mass density	ρ_f	kg/m^3	890.0	1,010.0
Specific heat capacity	c_f	J/(kg·K)	2,096.6	3,947.0
Thermal conductivity	λ_f	W/(m·K)	0.15	0.56
Kinematic viscosity	ν_f	mm^2/s	12.0	4.4
Dynamic viscosity	η_f	kg/(s·m)	0.011	0.004

position of the cutting fluid jet could be changed to guarantee a sufficient fluid supply.

Besides the difference between the mean and maximum temperature, Fig. 5 shows for both cutting fluids that with increasing cutting depth, the observed workpiece temperature increases as well. Yet, the observed workpiece temperature when applying the grinding oil is averagely about 41 % higher compared to the polymer dilution. This difference results from the different physical properties of both fluids. For example, the specific heat capacity of the polymer dilution is about 47 % lower than the grinding oil (Table 2). The heat created by the grinding process can be removed faster when applying the polymer dilution compared to the application of grinding oil. It also can be observed that the workpiece temperature distribution in the observed measurement field is more or less uniform and closely related to the mean temperature of the material removal process. Reason is the characteristic of the fast pendular movement of the grinding wheel and therefore the fast pendular movement of the heat source, resulting in a more or less uniform temperature distribution. The uniformity of the temperature distribution is also influenced by different physical properties of both fluids and the ability to dissipate the heat out of the workpiece.

When comparing the thermographic images, a darker background temperature is noticeable in case of the application of the polymer dilution. The reason of the darker background colour and lower temperature was a lower cutting fluid temperature compared to the grinding oil. The lower fluid temperature resulted in a lower temperature of the protective case by approximately 7 °C.

4.1.1 Specific grinding power and average surface roughness

Figure 6 presents the experimental results of the specific grinding power (chart (A), the average surface roughness (chart (B)) and the workpiece temperature measured with the infrared camera (chart (C)) and the thermocouples (chart (D)). The results are presented above an increasing cutting depth. For the comparison of the measurement results of the infrared camera and the thermocouples, the mean workpiece temperature in the centre of the thermographic image was used (compare Fig. 5 chart (B)), to comply with the mounting position of the thermocouples.

Table 3 Properties of the workpiece material (according to Rabiey [29])

Property	Symbol	Unit	Workpiece
Mass density	ρ_w	kg/m^3	7,810.0
Specific heat capacity	c_w	J/(kg·K)	461.0
Thermal conductivity	λ_w	W/(m·K)	39.6

The consideration of the specific grinding power in chart (A) and the average surface roughness in chart (B) shows an opposite behaviour. In case of the specific grinding power, the application of the grinding oil leads to considerably higher values than the use of the polymer dilution. The difference between both values increases further with inclining cutting depth. In case of the surface roughness, the values are initially comparable at a cutting depth of 5 μm when applying both cutting fluids. With inclining cutting depth the measured surface roughness increases. Yet, the application of the grinding oil results in a marginally better surface roughness than the polymer dilution.

The behaviour of the specific grinding power and the average surface roughness can be explained with a higher wear of the grinding wheel when applying the polymer dilution. The wear leads to the creation and engagement of new and sharp grains which generate few, but deep grooves on the workpiece surface [38]. Furthermore, the wear results in a lower effective cutting depth compared to the predefined cutting depth. Accordingly, the specific cutting power demand decreases Marinescu et al. [25]. A previous investigation focusing on the application of polymer dilution in comparison with grinding oil in external cylindrical grinding of 100Cr6 with aluminium oxide grinding wheel corresponds with this explanation [41].

The higher grinding wheel wear can be a result of the lower lubricity and the higher cooling capability of the polymer dilution compared to the grinding oil. A lower lubricity results in an increased friction and mechanical load on the bond and abrasive grain, whereby both splinter or break more easily. If the lubrication capability is too high, the grains rather blunt than splinter. In case of the cooling capability, the temperature gradient between grains/bond and the cutting fluid inclines with increasing cutting depth. In connection with a high cooling capability, thermal stress can occur within bond and

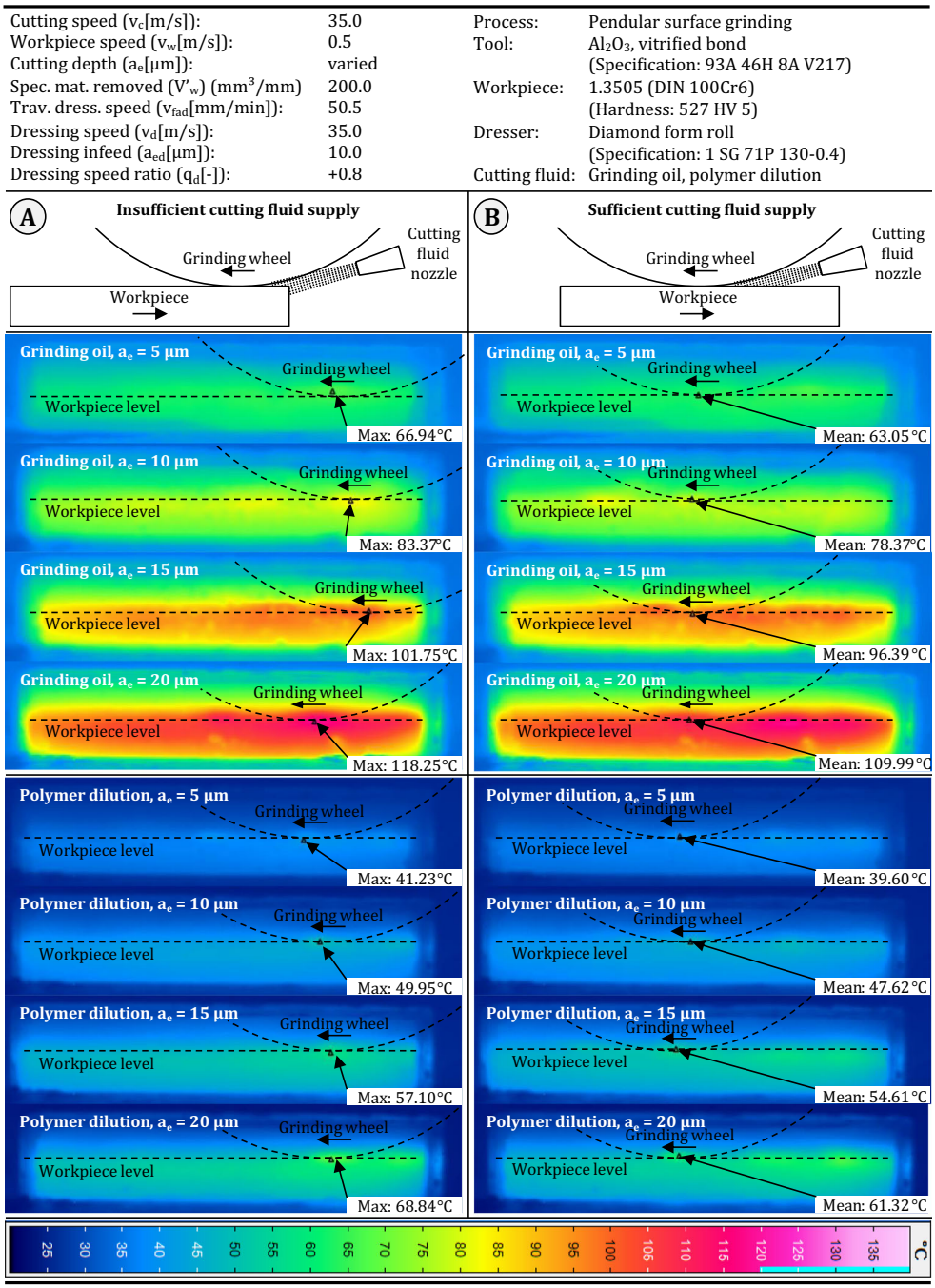

Fig. 5 Comparison of the maximal and mean workpiece side-plane temperature when applying grinding oil and polymer dilution (measured with an infrared camera)

grain, fostering an increased bond splintering and grain outbreaks [38, 41].

The measurement results with the infrared camera (chart (C)) and the thermocouples (chart (D)) show, as mentioned before, that the observed workpiece temperature, when applying the polymer dilution, is significantly lower compared to the usage of the grinding oil. The application of the thermoelements results in a lower observed workpiece temperature compared to the infrared camera. The reason could be the direct contact between the cutting fluid and the thermocouple resulting in cooling-down. To prevent this interference on the measurement, accuracy blind holes instead of through holes should be used.

4.2 Thermal analysis

Based on the equation presented in section 3.1 (see (Eq. 2) to (Eq. 14)), a thermal analysis was conducted. The results of the analysis are presented in Fig. 7. The figure shows in the upper two charts the comparison of the calculated convection heat transfer coefficients of grinding oil (chart (A)) and of the polymer dilution (chart (B)). The lower charts show a comparison

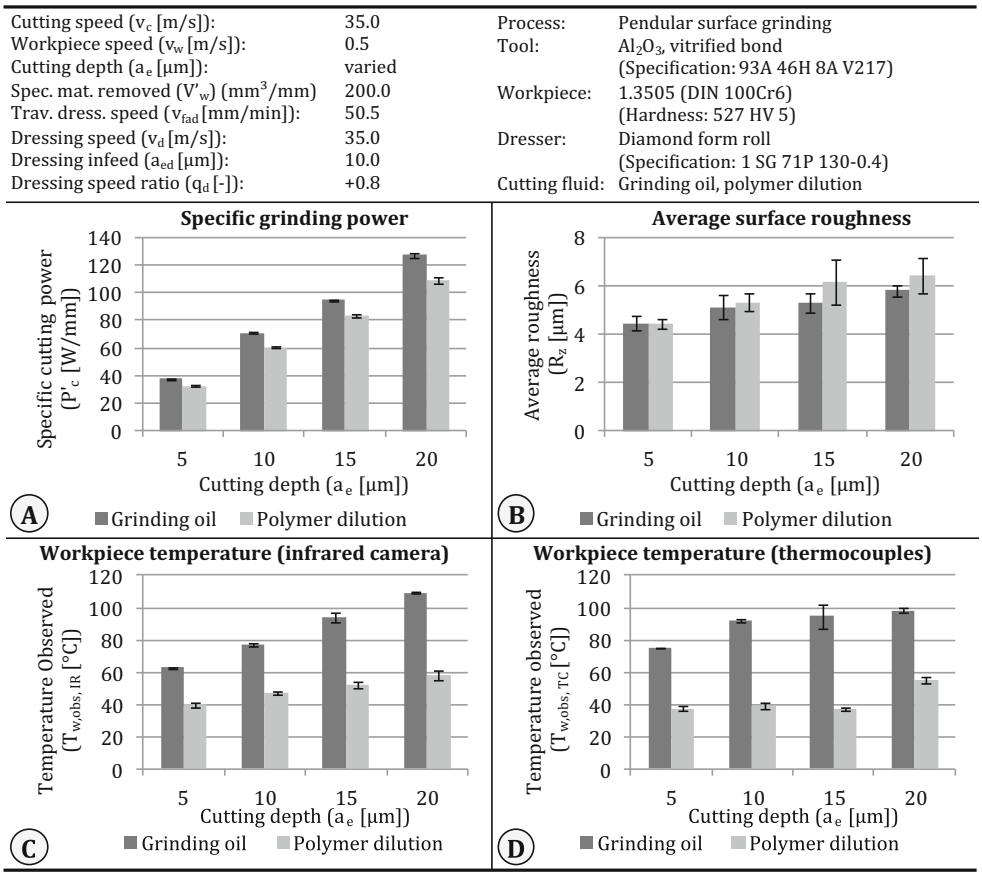

Fig. 6 Experimental results. Chart (**a**) specific grinding power, chart (**b**) average surface roughness, chart (**c**) workpiece temperature observed with infrared camera and chart (**d**) workpiece temperature observed with thermocouples

of the calculated and observed workpiece temperature when applying the grinding oil (chart (C)) and the polymer dilution (chart (D)).

The inversely determined convection heat transfer coefficient when applying the grinding oil was calculated with 52.81 kW/(m^2K) on average and when using the polymer dilution with 146.70 kW/(m^2K) on average. Similar values for non-water miscible and water miscible fluids were presented by Marinescu et al. [25].

The comparison of chart (A) and (B) indicates a major deviation between the heat transfer coefficient of the grinding oil and the polymer dilution. The reason for this deviation is due to the different fluid compositions and therefore different physical properties (see Table 2). The detailed comparison of the heat transfer coefficient in chart (A) or (B) show significant deviations between the inversely determined value (using (Eq. 14)) and the values calculated based on the two theoretical formulations. The experimentally observed value in charts (A) and (B) has the highest value followed by the value determined based on the formulation of Rowe and Zhang. In case of the formulation proposed by Zhang et al., the deviation is averagely 75 %, whilst in the case of the formulation presented by Rowe the deviation is averagely 7 %. However, a comparable deviation has been reported by Marinescu et al. [25]. Both analytical models show a decreasing heat for both fluids transfer coefficient with increasing cutting depth, due to the dependence of the analytical models on the cutting length.

As presented in charts (C) and (D) of Fig. 7, the application of the laminar flow model proposed by Zhang et al. could lead to a significant overestimation of the average workpiece temperature. In comparison, the usage of the fluid wheel model presented by Rowe results in a high accuracy.

The comparison of the calculated (based on the convection heat transfer coefficient formulated by Rowe) and the experimentally determined workpiece temperature in chart (C) and (D) show a good overall accuracy. An especially high accuracy can be determined between the calculated and the observed workpiece temperature using the infrared camera, whilst the comparison of the calculated and observed temperature using thermocouples show a good accuracy.

5 Conclusion

This study investigated the influence of the cutting fluid type on the average workpiece temperature. A non-water miscible grinding oil and a water miscible polymer dilution were compared in pendular surface grinding. The workpiece temperature was experimentally observed using an

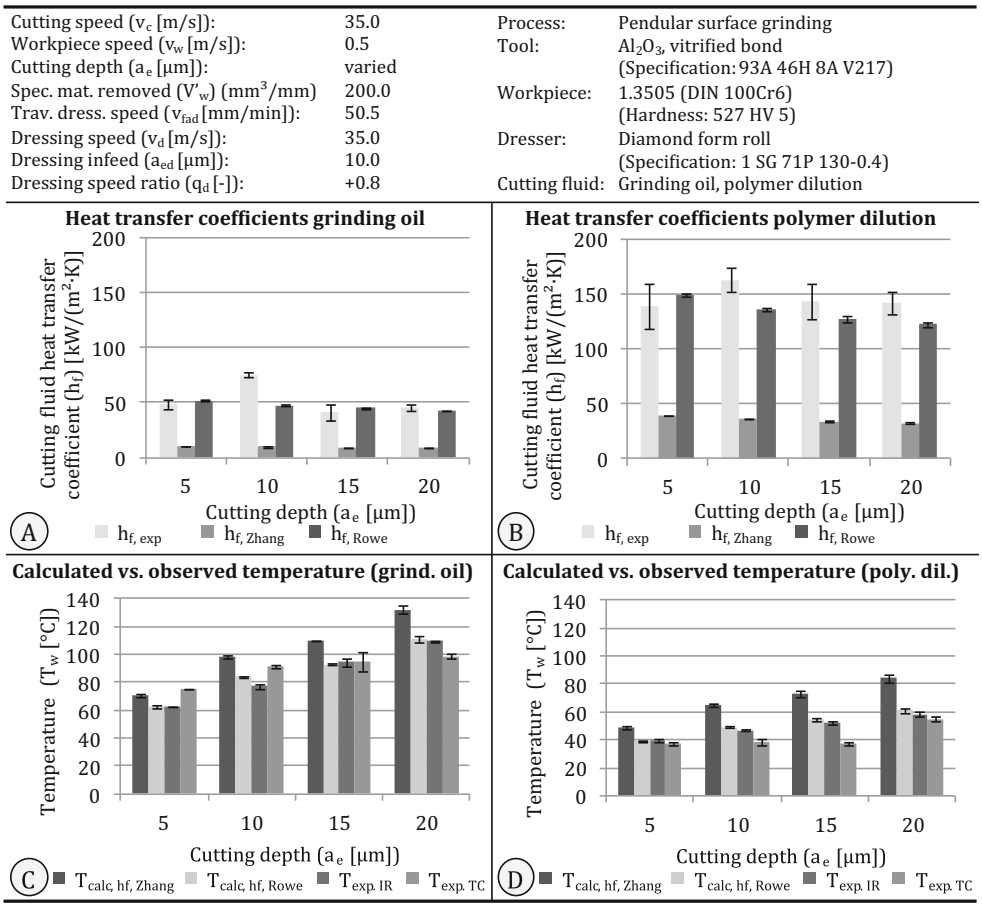

Fig. 7 Comparison of the theoretical and observed results. Heat transfer coefficient of the grinding oil (chart (**a**)) and polymer dilution (chart (**a**)) as well as calculated and observed workpiece temperature for grinding oil (chart (**c**)) and polymer dilution (chart (**d**)) (*IR* infrared camera, *TC* thermocouple)

infrared camera and thermocouples. Furthermore, the workpiece temperature was analytically calculated considering the influence of the cutting fluid's physical properties. Based on this investigation, the following conclusions can be drawn:

- The cooling properties of a mineral oil free, water miscible polymer dilution was firstly examined in comparison to a mineral oil-based grinding oil. The usage of the polymer dilution results in a lower average workpiece temperature and specific grinding power, but the achieved average workpiece surface was higher compared to the application of the grinding oil.
- The average workpiece temperature was successfully determined using an infrared camera. In comparison to the usage of thermocouples, the application of an infrared camera allowed to visualise the temperature field at the workpiece side-plane and the moving heat source created by the grinding process.
- An analytical thermal model of the average workpiece temperature was described considering the different fluids' physical properties and furthermore was verified with the observed values measured with the infrared camera and the thermocouples.
- The heat transfer coefficients of the cutting fluids were experimentally inversely determined and compared with the analytical models described in literature ("fluid wheel model" and the "laminar flow model"). Especially the "fluid wheel model" corresponds very well with the experimentally inversely determined values. In the experiments, the heat transfer coefficient of the grinding oil was inversely determined with averagely 52.81 kW/(m^2 K) and when using the polymer dilution averagely 146.70 kW/(m^2 K).

References

1. Anderson D, Warkentin A, Bauer R (2007) Comparison of numerically and analytically predicted contact temperatures in shallow and deep dry grinding with infrared measurements. Int J Mach Tools Manuf 48:320–328
2. Batako AD, Rowe WB, Morgan MN (2005) Temperature measurement in high efficiency deep grinding. Int J Mach Tools Manuf 45/11:1231–1245
3. Black SCE, Rowe WB, Qi HS, MiIls B (1996) Temperature measurement in grinding. MATADOR, Proceedings of the 31 St International Matador Conference Manchester, GB. 31:409–413

4. Black SCE (1996) The effect of abrasive properties on the surface integrity of ground ferrous materials. Ph.D. Thesis, Liverpool John Moores University. Liverpool, UK
5. Brandin H (1978) Pendelschleifen und Tiefschleifen Vergleichende Untersuchungen beim Schleifen von Rechteckprofilen (in German). Dr.-Ing. Dissertation, Technische Universität Braunschweig, Braunschweig, Germany
6. Carslaw H, Jaeger JC (2004) Conduction of heat in solids. Oxford Clarendon Press, Oxford
7. Choi H-Z (1986) Beitrag zur Ursachenanalyse der Randzonenbeeinflussung beim Schleifen (in German). Dr.-Ing. Dissertation, Universität Hannover, Germany
8. Comley P, Walton I, Jin T, Stephenson DJ (2006) A high material removal rate grinding process for the production of automotive crankshafts. CIRP Ann Manuf Technol 55/1:347–350
9. Dettmer T (2006) Nichtwassermischbare Kühlschmierstoffe auf Basis nachwachsender Rohstoffe (in German). Dr.-Ing. Dissertation, Technische Universität Braunschweig, Vulkan Verlag, Essen, Germany
10. Dederichs M (1972) Untersuchung der Wärmebeeinflussung des Werkstücks beim Flachschleifen (in German). Dr.-Ing. Dissertation, RWTH Aachen, Aachen, Germany
11. Denkena B, Tönshoff HK (2011) Spanen – Grundlagen, 3rd edn. Springer Verlag, Berlin
12. Hadad M, Sadeghi B (2012) Thermal analysis of minimum quantity lubrication—MQL grinding process. Int J Mach Tools Manuf 63:1–15
13. Hahn RS (1962) On the nature of the grinding process. Proceedings of 3rd Machine Tool Design and Research Conference. Birmingham, UK, pp 129–154
14. Heinzel C, Antsupov G (2012) Prevention of wheel clogging in creep feed grinding by efficient tool cleaning. CIRP Ann Manuf Technol 61/1:323–326
15. Jaeger JC (1942) Moving sources of heat and the temperature at sliding contacts. Proceedings, Royal Society, New South Wales, Australia. 76/3:203–224
16. Kato T, Fujii H (1997) Temperature measurement of workpiece in surface grinding by PVD film method. J Manuf Sci Eng 119:689–694
17. Lange D (1999) Meßsysteme und Regelkreise zur Qualitätsverbesserung und Erhöhung der Prozesssicherheit beim Schleifen mit CD (in German). Dr.-Ing. Dissertation, Technische Universität Braunschweig. Vulkan-Verlag, Essen, Germany
18. Langemeyer A (2002) Entwicklung und Bewertung von kühlschmierstofffreien Schleifsystemen beim Flachprofilschleifen (in German). Dr.-Ing. Dissertation, Technische Universität Braunschweig. Vulkan-Verlag, Essen, Germany
19. Lavine AS (2000) An exact solution for surface temperature in down grinding. Int J Heat Mass Transf 43:4447–4456
20. Lavine AS, Malkin S (1990) The role of cooling in creep feed grinding. Int J Adv Manuf Technol 5/2:97–111
21. Lin B, Morgan MN, Chen XW, Wang YK (2009) Study on the convection heat transfer coefficient of coolant and the maximum temperature in the grinding process. Int J Adv Manuf Technol 42/11-12:1175–1186
22. Maiz K (2008) Flachschleifen metallischer Werkstoffe unter Verwendung von flüssigem Stickstoff zur Kühlung (in German). Dr.-Ing. Dissertation, Technische Universität Braunschweig. Vulkan-Verlag, Essen, Germany
23. Malkin S, Guo C (2008) Grinding technology: theory and applications of machining with abrasives. Industrial Press, New York
24. Marinescu ID, Hitchiner M, Uhlmann E, Rowe WB, Inasaki I (2007) Handbook of machining with grinding wheels. Taylor & Francis Group, LLC, Boca Raton
25. Marinescu ID, Rowe WB, Dimitrov B, Ohmori H (2013) Tribology of abrasive machining processes. William Andrew Publishing, Norwich, USA
26. Meyer LW (2006) Einsatz von Temperatur und Kraftsensoren in Schleifwerkzeugen (in German). Dr.-Ing. Dissertation, Universität Bremen. Shaker Verlag, Aachen, Germany
27. Ohishi S, Furakawa Y (1985) Analysis of workpiece temperature and grinding burn in creep feed grinding. Bull Jpn Soc Mech Eng 28/242:1775–1781
28. Outwater JO, Shaw MC (1952) Surface temperature in grinding. Trans ASME 74/1:73–83
29. Rabiey M (2010) Dry Grinding with cBN Wheels – The effect of structuring. Dr.-Ing. Dissertation, Universität Stuttgart, Stuttgart, Germany
30. Rowe WB (2009) Principles of modern grinding technology. William Andrew, Elsevier, Oxford
31. Saljé E (1991) Begriffe der Schleif- und Konditioniertechnik. Vulkan Verlag, Essen
32. Schwarz F (2010) Simulation der Wechselwirkungen zwischen Prozess und Struktur bei der Drehbearbeitung. Dr.-Ing. Dissertation, Technische Universität München, München, Germany
33. Tönshoff HK, Friemuth T, Becker JC (2002) Process monitoring in grinding. CIRP Ann Manuf Technol 51(2):551–571
34. Tönshoff HK, Denkena B (2013) Basics of cutting and abrasive processes. Springer Verlag, Berlin
35. Ueda T, Hosokawa A, Yamamoto A (1985) Studies on temperature of abrasive grain in grinding-application of infrared radiation pyrometer. J Eng Ind 107:127–133
36. Ueda T, Tanaka H, Torii A, Sugita T (1993) Measurement of grinding temperature of active grains using infrared radiation pyrometer with optical fiber. CIRP Ann Manuf Technol 42(1):405–408
37. Ueno T, Ishibashi A, Katsuki A (1970) Experiments on the cooling ability of cutting fluids. Bull Jpn Soc Mech Eng 13(59):729–736
38. Vits R (1985) Technologische Aspekte der Kühlschmierung beim Schleifen (in German). Dr.-Ing. Dissertation, RWTH Aachen, Aachen, Germany
39. Weber T (2001) Simulation des Flachprofilschleifens mit Hilfe der Finite-Elemente-Methode (in German). Dr.-Ing. Dissertation, Technische Universität Braunschweig. Vulkan-Verlag, Essen, Germany
40. Werner G (1971) Kinematik und Mechanik des Schleifprozesses (in German). Dr.-Ing. Dissertation, RWTH Aachen, Aachen, Germany
41. Winter M, Bock R, Herrmann C (2013) Investigation of a new polymer-water based cutting fluid to substitute mineral oil based fluids in grinding processes. CIRP J Manuf Sci Technol 6(4):254–262
42. Winter M, Herrmann C (2014) Eco-efficiency of alternative and conventional cutting fluids in external cylindrical grinding. Procedia CIRP 15:68–73
43. Wittmann M (2007) Bedarfsgerechte Kühlschmierung beim Schleifen (in German). Dr.-Ing. Dissertation, Universität Bremen. Shaker Verlag, Aachen, Germany
44. Xu X, Malkin A (2001) Comparison of methods to measure grinding temperatures. J Manuf Sci Eng 123:191–195
45. Yasui H, Tsukuda S (1983) Influence of fluid type on wet grinding temperature. Bull Jpn Soc Mech Eng 17/2:133–134
46. Zhang L, Rowe WB, Morgan MN (2013) An improved fluid convection solution in conventional grinding. Proc Inst Mech Eng B J Eng Manuf 227/6:832–838
47. Zhu D Li B, Ding H (2013): An improved grinding temperature model considering grain geometry and distribution. The International Journal of Advanced Manufacturing Technology. 67/5:1393–1406